

Article

Inhibition of Mild Steel Corrosion by 4-benzyl-1-(4-oxo-4-phenylbutanoyl)thiosemicarbazide: Gravimetical, Adsorption and Theoretical Studies

Ahmed A. Alamiery ^{1,2,*} , Wan Nor Roslam Wan Isahak ²  and Mohd S. Takriff ³

¹ Department of Chemical and Process Engineering, Faculty of Engineering and Built Environment, Universiti Kebangsaan Malaysia (UKM), P.O. Box 43000, Bangi 43600, Malaysia

² Energy and Renewable Energies Technology Center, University of Technology, Baghdad 10001, Iraq; wannorroslam@ukm.edu.my

³ Chemical and Water Desalination Engineering Program, Collage of Engineering, University of Sharjah, Sharjah 26666, United Arab Emirates; sobritakriff@ukm.edu.my

* Correspondence: dr.ahmed1975@gmail.com or dr.ahmed1975@ukm.edu.my

Abstract: Gravimetric measurements were applied to study the inhibitory effect of 4-benzyl-1-(4-oxo-4-phenylbutanoyl)thiosemicarbazide (BOT) on the corrosion of mild steel in 1.0 M HCl. BOT has a good inhibitory efficacy of 92.5 percent at 500 ppm, according to weight loss results. The effect of inhibitor concentration on the mild corrosion behavior of steel was investigated and it was discovered that the higher the inhibitor concentration, the higher the damping efficiency. The results confirm that BOT is an effective corrosion inhibitor for mild steel in the presence of 1.0 M HCl. Furthermore, the higher protection efficiency with increasing temperature and the free energy value showed that BOT molecules participate in both chemisorption (coordination bonds between the active sites of BOT molecules and d-orbital of iron atoms) and physisorption (through the physical interactions on the mild steel surface). The adsorption mechanism on the mild steel surface obeys the Langmuir adsorption isotherm model. Quantum chemical calculations based on the DFT calculations were conducted on BOT. DFT calculations indicated that the protective efficacy of the tested inhibitor increased with the increase in energy of HOMO. The theoretical findings revealed that the broadly stretched linked functional groups (carbonyl and thionyl) and heteroatoms (sulfur, nitrogen and oxygen) in the structure of tested inhibitor molecules are responsible for the significant inhibitive performance, due to possible bonding with Fe atoms on the mild steel surface by donating electrons to the d-orbitals of Fe atoms. Both experimental and theoretical findings in the current investigation are in excellent harmony.



Citation: Alamiery, A.A.; Wan Isahak, W.N.R.; Takriff, M.S. Inhibition of Mild Steel Corrosion by 4-benzyl-1-(4-oxo-4-phenylbutanoyl)thiosemicarbazide: Gravimetical, Adsorption and Theoretical Studies. *Lubricants* **2021**, *9*, 93. <https://doi.org/10.3390/lubricants9090093>

Received: 27 July 2021

Accepted: 5 September 2021

Published: 15 September 2021

Keywords: corrosion inhibition; phenylbutanoyl; HCl; weight loss; DFT

Publisher's Note: MDPI stays neutral with regard to jurisdictional claims in published maps and institutional affiliations.



Copyright: © 2021 by the authors. Licensee MDPI, Basel, Switzerland. This article is an open access article distributed under the terms and conditions of the Creative Commons Attribution (CC BY) license (<https://creativecommons.org/licenses/by/4.0/>).

1. Introduction

Mild steel is frequently used in a variety of industrial environments. Due to the strength of its impact, this material has been used in a variety of fields [1]. On the other hand, cleaning, pickling and descaling cause its corrosion [2]. In a variety of industrial processes, acid solutions are commonly used to remove unwanted deposits and rust [3]. To achieve this, it must be protected from unexpectedly occurring metal disintegration [4]. Inhibitors are among the most effective strategies for protection against corrosion, especially in acidic environments where alloys are at risk of melting [5]. Due to their biodegradable ability, environmental friendliness, low cost and availability, investigators have recently focused on the use of environmentally acceptable chemicals, such as natural and synthetic organic compounds [6]. Organic molecules employed as corrosion inhibitors produce coordination complexes with a metallic surface utilizing the active sites, and these metallic complexes occupy a significant surface area, therefore coating the metallic surface and

shielding it from acidic solutions [7]. Due to their exposure to various corrosive conditions, many metals and alloys utilized in various human activities are susceptible to various corrosion mechanisms [8]. Mild steel is one of the most essential of these alloys [9]. The inclusion of inhibitors is one of the strategies for reducing the rate of metal corrosion [10–12]. Many investigations have been carried out in order to develop chemicals that can be used as corrosion inhibitors for this metal in various aqueous conditions [13]. In the current study, the impact of 4-benzyl-1-(4-oxo-4-phenylbutanoyl)thiosemicarbazide (BOT) as a corrosion inhibitor of carbon steel in 1 M HCl has been regularly examined by gravimetric techniques. Experimental findings are described and explained. The inhibitor BOT used in this investigation has a large number of donating atoms (nitrogen, oxygen and sulfur atoms). The utilized inhibitor's molecular structure is shown in Figure 1.

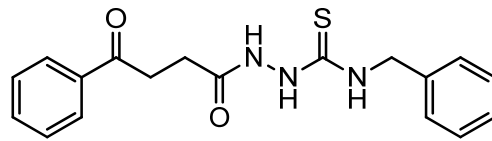


Figure 1. Structure of 4-benzyl-1-(4-oxo-4-phenylbutanoyl)thiosemicarbazide (BOT).

2. Materials and Methods

2.1. Corrosive Media

The corrosive environment in the investigations was a 1 M hydrochloric acid solution which was made from an analytical reagent grade of HCl 37 percent and double-distilled water.

2.2. Weight Loss Investigations

The analyses were conducted in the environment of 1 M HCl (in the absence and in presence of tested corrosion inhibitor) on mild steel coupon with the composition of 0.210% carbon, 0.050% manganese, 0.380% silicon, 0.010% aluminum, 0.050% sulfur, 0.090% phosphorus and balance iron. Coupons with dimensions $45 \times 25 \times 0.2$ mm were applied. The coupons were sanded several times with various grades of sandpaper, up to 1200 grades. Each test was conducted in a 250 mL beaker having 100 mL 1M HCl as a corrosive environment. A clean coupon was weighed and exposed to corrosive solution. After 1, 5, 10, 24 and 48 h of exposure period in 1 M HCl solution in absence and presence of tested inhibitor at various concentrations (100, 200, 300, 400, 500 and 1000 ppm), the coupon was removed, soaked with double-distilled water, washed with acetone, dried in oven and weighed by electronic balance. The rate of corrosion rate (C_R ; mmy^{-1}) and protection efficiency ($IE\%$) were determined from gravimetric measurements based on Equations (1) and (2) respectively [14,15].

$$C_R = \frac{87.6w}{atd} \quad (1)$$

$$IE\% = \frac{w_o - w_i}{w_o} \times 100 \quad (2)$$

2.3. Effect of Temperature

The analysis coupons of chosen thickness have been conducted for the temperature investigation at 303, 313, 323 and 333 K. The tested coupons with dimensions $45 \times 25 \times 0.2$ mm³ were applied. Each test was conducted in a 250 mL beaker having 100 mL 1 M HCl as a corrosive environment. A clean coupon was weighed and exposed to the corrosive solution. After 5 h of exposure time in 1 M HCl solution in absence and presence of tested inhibitor at various concentrations (100, 200, 300, 400, 500 and 1000 ppm), and different investigated temperature at 303, 313, 323 and 333 K, the coupon was removed, soaked with double-distilled water, washed with acetone, dried in the oven and weighed by electronic balance. All weight loss experiments were repeated three times.

2.4. Computational Details

To calculate the ground-state geometries, Gaussian 03, Revision C.01 was optimized to a local minimum without symmetry restrictions using the valence and polarization basis set (6-31G++(d,p)). A combination of the Becke three-parameter hybrid (B3) exchange functional and the Lee–Yang–Parr (LYP) correlation functional (B3LYP), a version of the (DFT) method was used in gas phase to determine all optimized geometries, *HOMO* energies (E_{HOMO}), *LUMO* energies (E_{LUMO}) and physical properties (for the molecules in this study). The *HOMO*, *LUMO*, ΔE , η , σ , χ and ΔN were calculated using Equations (3)–(7) [16,17].

$$\Delta E = E_{HOMO} - E_{LUMO} \quad (3)$$

$$\eta = -\frac{E_{HOMO} - E_{LUMO}}{2} \quad (4)$$

$$\sigma = \frac{1}{\eta} \quad (5)$$

$$\chi = -\frac{E_{HOMO} + E_{LUMO}}{2} \quad (6)$$

$$\Delta N = \frac{\chi_{Fe} - \chi_{inh}}{2(\eta_{Fe} + \eta_{inh})} \quad (7)$$

where χ_{Fe} and η_{Fe} were 7 eV/mol and 0 eV/mol, respectively.

3. Results and Discussion

3.1. Weight Loss Techniques

The corrosion rate and protection efficiency values were determined from mass loss techniques at various concentrations of BOT in 1.0 M HCl after immersion periods (1, 5, 10, 24 and 48 h), at 303 K. The experimental results are demonstrated in Figures 2 and 3. It was noted that BOT controls and/or retarding the mild steel corrosion in 1.0 M corrosive environments at different concentrations were applied in the investigation. Certainly, the mild steel rate of corrosion values decreased from 24.25 to 6.86 mmy^{-1} on the increase in the inhibitor concentration from 100 to 500 ppm as appears in Figure 2. It is obvious from Figure 3 that the protection performance increased from 48.9 to 96.274.8% in presence of 100 to 500 ppm of BOT at 5 h as immersion time. The highest inhibitive efficacy was determined at 1000 ppm concentration of BOT and additional increasing concentration of BOT did not increase inhibition efficiency. The inhibition efficiency at the inhibitor concentration 500 ppm was 96.2%; this value had no significant change compared with the inhibition efficiency at the inhibitor concentration 1000 ppm, which was 96.7% at 5 h as immersion time. The effect of higher adsorption and greater covering of BOT molecules on the mild steel surface with increasing BOT concentration could explain the improved inhibition efficiency and reduced corrosion rate [18,19].

3.2. Effect of Immersion Time

The difference of inhibitive efficacy with different exposure periods times from 1.0 h to 48.0 h at various BOT concentrations is also presented in Figure 3. At the concentration of 500 ppm, the inhibition efficiency increased from 77.8 to 96.2% when the exposure period increased from 1 to 5 h, and from 5 to 10 h, no significant differences in inhibition efficiency were noted (96.2–96.8%). These results were attributed to the increased rate of metal corrosion as exposure time increases. It is obvious that BOT inhibited mild steel corrosion in a 1 M HCl environment [20]. Furthermore, the inhibition efficiency decreased from 96.8 to 77.9% when the exposure period increased from 10 to 48 h.

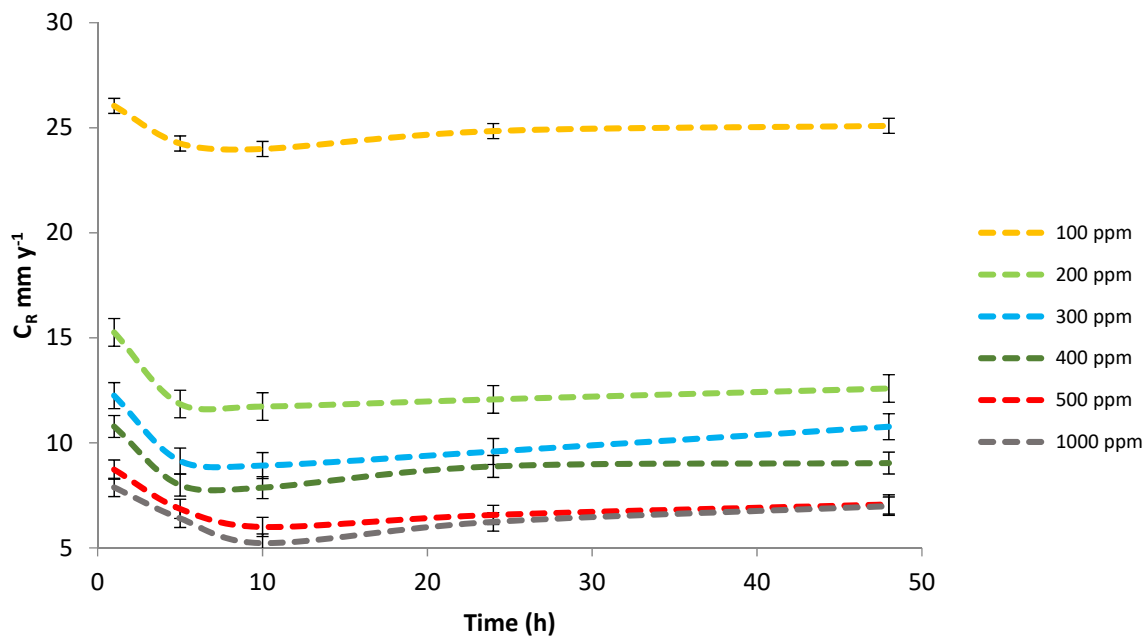


Figure 2. Difference of corrosion rate in 1 M HCl on the surface of mild steel with various exposure times.

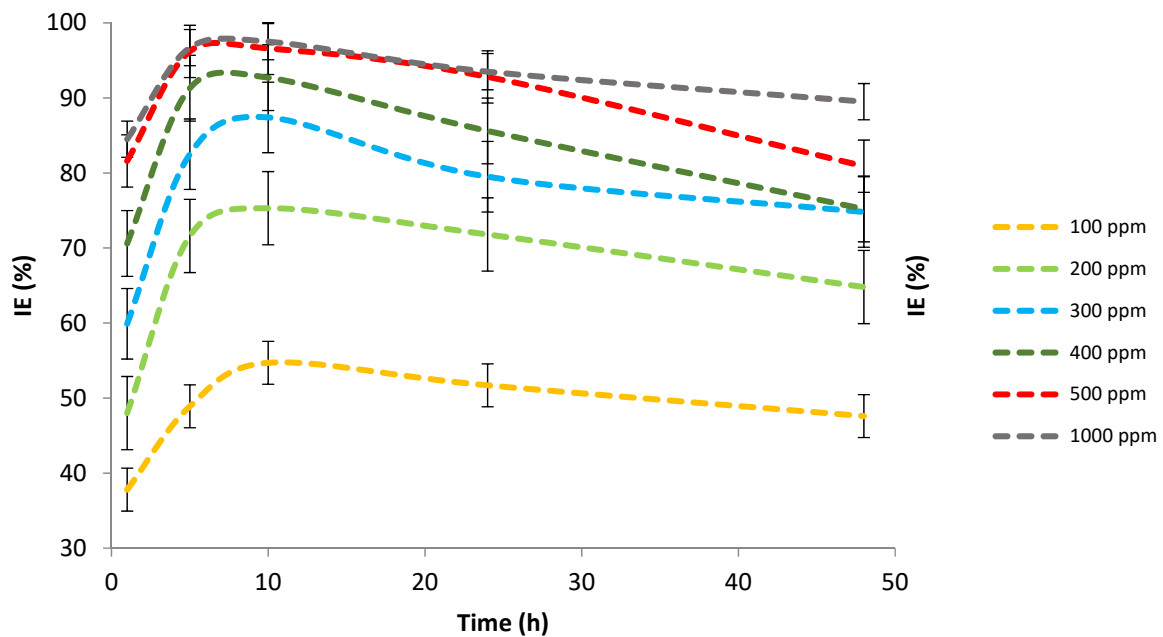


Figure 3. Difference of inhibitive efficiency in 1 M HCl on the surface of mild steel with various exposure times.

3.3. Effect of Temperature

Temperature can vary the interaction between the mild steel surface and the corrosive environment in the absence and presence of a tested inhibitor (BOT). The corrosion rate and protection efficiency values obtained from weight loss measurements for mild steel in 1 M HCl in the presence of various concentrations of BOT at the temperature range 303–333 K are postulated in Figure 4. The weight loss findings show that the corrosion rate increased with raising the temperature in the presence of various inhibitor concentrations for 5 h as immersion time. In the presence of BOT molecules, the surface coverage (θ), determined by $IE/100$, reduced lightly with rising temperature, which might be owing to the desorption of the BOT molecules from the mild steel surface. The insignificant reduction of surface coverage implies that the protection performance of BOT is temperature independent. Hence, BOT works as an effective inhibitor in the range of temperature investigated [18–21].

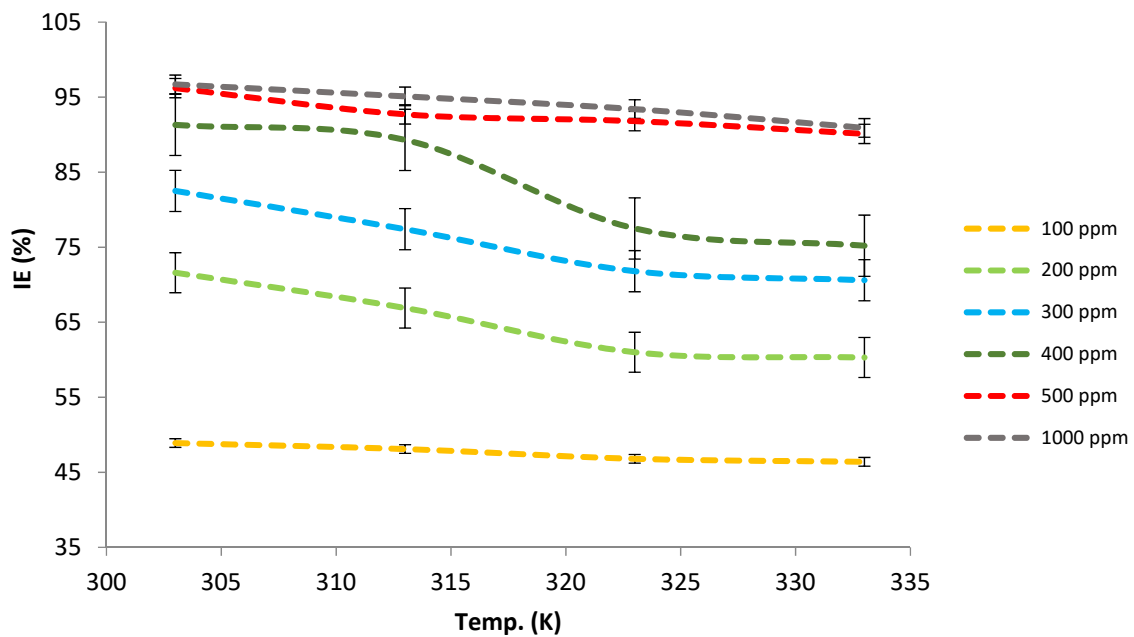


Figure 4. Difference of inhibitive efficiency in 1 M HCl on the surface of mild steel with various temperature.

3.4. Adsorption Isotherm

The adsorption isotherm subject indicates the interactions between inhibitor molecules and metal surface. The surface coverage (θ) values at various inhibitor concentrations in 1 M hydrochloric acid solution were computed for this goal. Temkin and Langmuir adsorption isotherm models are the most often utilized isotherms. Efforts to fit weight loss measurement data into various adsorption isotherms revealed that the data best fit the Langmuir adsorption isotherm. Langmuir hypotheses relate the concentration of the inhibitor in the corrosive solution (C_{inh}) to the surface coverage degree according to Equation (8),

$$\frac{C_{inh}}{\theta} = \frac{1}{K_{ads}} + C_{inh} \quad (8)$$

where, K_{ads} represents the adsorption equilibrium constant.

The linear regression parameter (R^2) between C_{inh}/θ and C_{inh} is 0.9995, as in Figure 5. Figure 5 exhibits the straight line of C_{inh}/θ against C_{inh} at 303 K. These findings confirm that the (R^2) and slope are equal to 1, which approves the adsorption of BOT molecules on the surface of mild steel follows Langmuir isotherms. The slope of the C_{inh}/θ against C_{inh} plot displays a difference from unity, which indicates non-ideal simulating [21,22] and unexpected from the Langmuir isotherms. It might be the outcomes from the interactions between the adsorbed BOT molecules on the tested metal surface [23,24].

K_{ads} and ΔG_{ads}^0 (adsorption free energy) were determined according to Equation (9),

$$\Delta G_{ads}^0 = -RT \ln(55.5 K_{ads}) \quad (9)$$

where, 55.5 represents the water concentration (mol L^{-1}) and R is the gas constant.

Usually, the value of ΔG_{ads}^0 about -20 kJ mol^{-1} or below is compatible with the physisorption and if it is about -40 kJ mol^{-1} or higher value then this is chemisorption [25]. Here, the determined ΔG_{ads}^0 value is $-37.1 \text{ kJ mol}^{-1}$ symbolizing that the mechanism of adsorption of BOT on mild steel in 1 M HCl solution at 303 K is both chemical interaction and electrostatic interaction. ΔG_{ads}^0 with negative value assuring the inhibitor molecule which adsorbed onto the surface of mild steel is a spontaneous process.

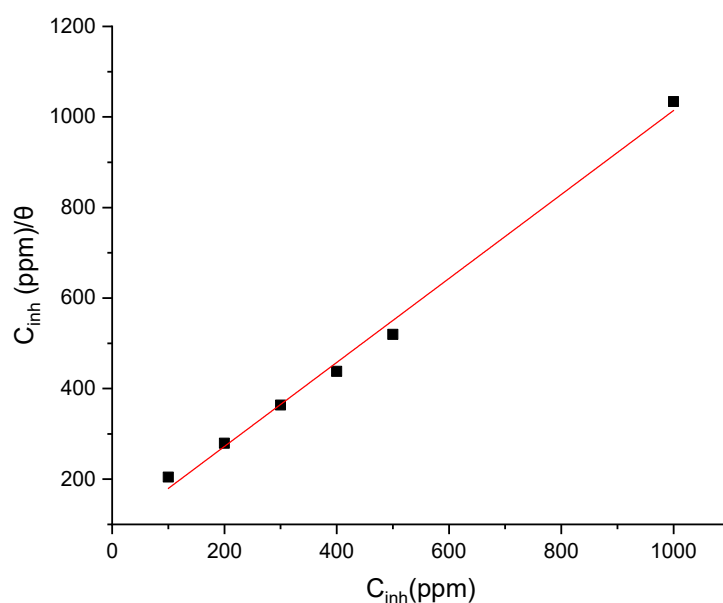


Figure 5. Langmuir adsorption isotherm model for the adsorption of BOT in 1 M HCl on the surface of mild steel.

3.5. Theoretical Calculation

Quantum chemical investigations have been performed to compare the corrosion inhibition efficacy of the tested inhibitor molecules with the computed frontier molecular orbital (FMO) energy levels. Moreover, the quantum chemical computations results could be achieved without lab analyses, therefore avoiding wasting time and material [26]. Quantum chemical parameters determined from the computations which are efficient for the protection performance of tested inhibitor molecules, such as the FMOs energies (E_{HOMO} and E_{LUMO}), the energy of separation ($E_{LUMO} - E_{HOMO}$), ΔE , describing the reactivity function, the net charge on the functional group, dipole moment and total energy, are collected in Table 1. The E_{HOMO} describes a molecule's ability to donate a lone pair of electrons; the higher the E_{HOMO} value, the greater the molecule's tendency to donate electrons to an electrophilic reagent, while the lower the E_{LUMO} , the greater the molecule's tendency to accept electrons from iron atoms. The energy variation between E_{HOMO} and E_{LUMO} informs on the reactivity of the given chemical; the smaller the ΔE value, the greater the reactivity of the molecule, as seen in Table 1. When compared to several previously published molecules, the results demonstrate that BOT has the lowest ΔE value (2.608 eV) and is thus the most reactive molecule [27]. The polarity is determined by the dipole moment. The polarity of a molecule is proportional to its dipole moment [28]. The orbital electron energies were spread uniformly across the molecules, according to the BOT's $HOMO$ and $LUMO$ diagrams (Figure 6a–c).

Table 1. Quantum chemical parameters of BOT.

E_{HOMO} (eV)	E_{LUMO} (eV)	$\Delta E = (E_{HOMO} - E_{LUMO})$	η	σ	χ	(ΔN)	μ (D)	IE (%) *
−7.284	−4.676	−2.608	1.304	0.7668	5.98	0.3911	7.0311	96.2

* IE (%) values were calculated from weight loss measurement.

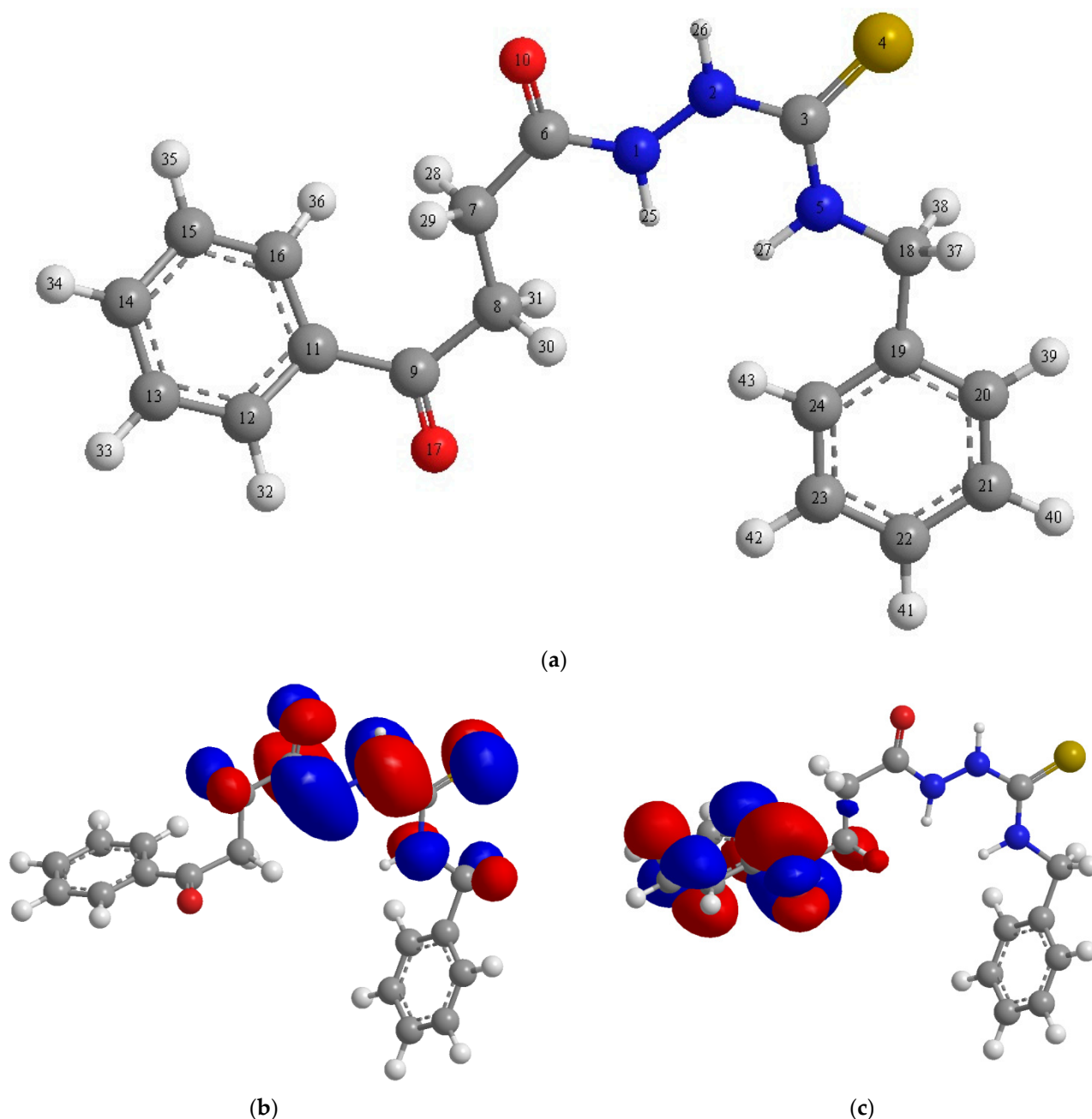


Figure 6. (a) Optimized structure, (b) HOMO structure, (c) LUMO structure.

The global hardness (η), softness (σ), electronegativity (χ) and the fraction of electron transfer (ΔN) collectively describe the dynamic parameters that are calculated, as presented in Table 1. In the estimation of the specified chemical parameters, Koopmans' theorem [17] presents excellent abilities to theoretical and computational researchers. Based on this theory, the values of electron affinity and ionization energy of chemical species are connected with values of $EHOMO$ and $ELUMO$. The principle of hard–soft acid and base (HSAB) [29,30] presented by Pearson declares that “hard acids prefer to coordinate to hard bases and soft acids prefer to coordinate to soft bases”. As can be understood from Pearson's classification, nitrogen-containing structure contributes its electrons readily to the d-orbital of iron atoms on the surface of mild steel [31]. As a result, the soft molecule has adsorption capability owing to its easier electron transfer and excellent corrosion inhibitor than the hard one. As per Lukovit's research, when the number of electrons transmitted (ΔN) is less than 3.6, the inhibitory effectiveness as a function of electron

transfer improves [17]. The better the corrosion inhibitor, the higher the electron transfer fraction (ΔN).

3.6. Mulliken Charges

The investigated inhibitor is studied using the DFT Mulliken charges, which is an indication of reactive molecular centers. The Mulliken charge measurement is important for determining inhibitor adsorption sites. The capacity to be adsorbed on the metallic surface increases as the negatively charged heteroatom becomes more negatively charged. Higher negative charges are detected around nitrogen, sulphur, oxygen and some carbon atoms in BOT, indicating that these are the inhibitors' coordinating sites. The nitrogen bonded as N-Thioamide and N-thioamide, and also the oxygen bonded as O-Carbonyl, whereas the sulfur linked to the mild steel surface atoms as S-Thiocarbonyl, on the other hand, indicates that greater negative Mulliken charges were chosen for the bonding sites. Table 2 summarizes the Mulliken charges. As a result, the more negative the Mulliken atomic charge of the tested inhibitor, the easier it is for the atom to donate its electrons to the metal's unoccupied orbital and adsorbs preferentially on the metal surface, forming a densely packed adsorption layer that prevents metal ions from entering the solution. Three nitrogen atoms N-Thioamide (−0.7301), N Amide (−0.43) and N Amide (−0.43) and two oxygen atoms in the oxo groups O- Carbonyl (−0.57) and O- Carbonyl (−0.57) and Thiocarbonyl group (Thiocarbonyl (−0.38), all of which have higher negative charges, might carry electrons to the d-orbital of iron atoms on the mild steel surface to form coordination bonds, as explained in Figure 6.

Table 2. The Mulliken charges of BOT molecules.

Atom	Charge	Atom	Charge	Atom	Charge	Atom	Charge
N(1)	−0.524240	C(7)	−0.495498	C(13)	−0.184849	C(19)	−0.000172
N(2)	−0.503825	C(8)	−0.479102	C(14)	−0.174124	C(20)	−0.182332
C(3)	0.244554	C(9)	0.447670	C(15)	−0.180262	C(21)	−0.180628
S(4)	−0.050101	O(10)	−0.486797	C(16)	−0.205481	C(22)	−0.187090
N(5)	−0.699234	C(11)	−0.092317	O(17)	−0.452130	C(23)	−0.177991
C(6)	0.668898	C(12)	−0.147503	C(18)	−0.209222	C(24)	−0.202524

4. Conclusions

Based on the experimental findings the resulting conclusions can be expressed.

1. The organic compound 4-benzyl-1-(4-oxo-4-phenylbutanoyl)thiosemicarbazide (BOT) was studied as an inhibitor for corrosion of mild steel in 1 M environment.
2. The experimental findings achieved point to the result that BOT efficiently controls or retards the mild steel corrosion in 1.0 M hydrochloric acid solution.
3. With increasing BOT concentration, inhibitive effectiveness increases and the rate of corrosion decreases in HCl solution.
4. The inhibition efficiency decreases slightly with the increase in the temperature in HCl solution.
5. The process of corrosion was controlled by the adsorption of the BOT molecules on the metallic surface.
6. Adsorption of BOT molecules on the examined metallic surface from acidic solution follow the Langmuir isotherms model.
7. The adsorption of BOT molecules on the surface of mild steel involving both chemisorption and physisorption.
8. The DFT theoretical results on BOT were investigated. The calculation results demonstrate the tested inhibitor is considered a promising and important corrosion inhibitor compared to other published corrosion inhibitors. The quantum chemical parameters, including frontier molecular orbitals (*HOMO* and *LUMO*), dipole moment (μ),

absolute electronegativity (χ), global hardness (η), softness (σ) and the fraction of electrons transferred (ΔN), have been determined at the B3LYP level of theory with 6-31G(d,p) basis set. The obtained parameters support the validity of the quantum chemical approach used in this study. According to quantum chemical calculations, the examined inhibitor has the strongest affinity to adsorb onto the metal surface compared to other published corrosion inhibitors.

9. The synthesized inhibitor is believed to exhibit good protection against corrosion in a hydrochloric acid environment. The major disadvantage is the time dependence of percent inhibition efficiency (%IE) of the tested inhibitor.

Author Contributions: Conceptualization, A.A.A.; methodology, A.A.A. and W.N.R.W.I. software, A.A.A.; validation, W.N.R.W.I. and M.S.T.; investigation, A.A.A. and W.N.R.W.I.; resources, W.N.R.W.I. and M.S.T.; data curation, A.A.A.; writing—original draft preparation, A.A.A.; writing—review and editing, A.A.A.; visualization, M.S.T.; supervision, A.A.A. All authors have read and agreed to the published version of the manuscript.

Funding: This research received no external funding.

Data Availability Statement: The data of this study are available from the corresponding author (A.A.A.), upon reasonable request.

Acknowledgments: The authors thank Universiti Kebangsaan Malaysia (Malaysia) and University of Technology (Iraq) for supporting this work.

Conflicts of Interest: The authors declare no conflict of interest.

References

1. Guo, L.; Obot, I.B.; Zheng, X.; Shen, X.; Qiang, Y.; Kaya, S.; Kaya, C. Theoretical insight into an empirical rule about organic corrosion inhibitors containing nitrogen, oxygen, and sulfur atoms. *Appl. Surf. Sci.* **2017**, *406*, 301–306. [[CrossRef](#)]
2. Saha, S.K.; Hens, A.; Murmu, N.C.; Banerjee, P. A comparative density functional theory and molecular dynamics simulation studies of the corrosion inhibitory action of two novel N-heterocyclic organic compounds along with a few others over steel surface. *J. Mol. Liq.* **2016**, *215*, 486–495. [[CrossRef](#)]
3. Verma, C.; Verma, D.K.; Ebense, E.E.; Quraishi, M.A. Sulfur and phosphorus heteroatom-containing compounds as corrosion inhibitors: An overview. *Heteroat. Chem.* **2018**, *29*, e21437. [[CrossRef](#)]
4. Fergachi, O.; Benhiba, F.; Rbaa, M.; Ouakki, M.; Galai, M.; Tour, R.; Lakhri, B.; Oudda, H.; Touhami, M.E. Corrosion Inhibition of Ordinary Steel in 5.0 M HCl Medium by Benzimidazole Derivatives: Electrochemical, UV-Visible Spectrometry, and DFT Calculations. *J. Bio-Tribo-Corros.* **2019**, *5*, 21. [[CrossRef](#)]
5. Ahmed, S.K.; Ali, W.B.; Khadom, A.A. Synthesis and Characterization of New Triazole Derivatives as Corrosion Inhibitors of Carbon Steel in Acidic Medium. *J. Bio-Tribo-Corros.* **2018**, *5*, 1–17. [[CrossRef](#)]
6. Kumar, H.; Dhanda, T. Application of 1,2,3-Benzotriazole as Corrosion Inhibitor for Mild Steel in Sulphuric Acid Medium at Different Temperature. *Asian J. Chem.* **2019**, *32*, 153–160. [[CrossRef](#)]
7. Gopi, D.; Sherif, E.-S.M.; Manivannan, V.; Rajeswari, D.; Surendiran, M.; Kavitha, L. Corrosion and Corrosion Inhibition of Mild Steel in Groundwater at Different Temperatures by Newly Synthesized Benzotriazole and Phosphono Derivatives. *Ind. Eng. Chem. Res.* **2014**, *53*, 4286–4294. [[CrossRef](#)]
8. El-Shafei, A.; Moussa, M.; El-Far, A. The corrosion inhibition character of thiosemicarbazide and its derivatives for C-steel in hydrochloric acid solution. *Mater. Chem. Phys.* **2001**, *70*, 175–180. [[CrossRef](#)]
9. Ebense, E.E.; Isabirye, D.A.; Eddy, N.O. Adsorption and quantum chemical studies on the inhibition potentials of some thiosemicarbazides for the corrosion of mild steel in acidic medium. *Int. J. Mol. Sci.* **2010**, *11*, 2473–2498. [[CrossRef](#)]
10. Badr, G. The role of some thiosemicarbazide derivatives as corrosion inhibitors for C-steel in acidic media. *Corros. Sci.* **2009**, *51*, 2529–2536. [[CrossRef](#)]
11. Obayes, H.R.; Alwan, G.H.; Alobaidy, A.H.M.; Al-Amiery, A.A.; Kadhum, A.A.H.; Mohamad, A.B. Quantum chemical assessment of benzimidazole derivatives as corrosion inhibitors. *Chem. Cent. J.* **2014**, *8*, 21. [[CrossRef](#)]
12. Ansari, K.; Quraishi, M.; Singh, A. Schiff's base of pyridyl substituted triazoles as new and effective corrosion inhibitors for mild steel in hydrochloric acid solution. *Corros. Sci.* **2014**, *79*, 5–15. [[CrossRef](#)]
13. Lgaz, H.; Salghi, R.; Bhat, K.S.; Chaoui, A.; Shubhalaxmi; Jodeh, S. Correlated experimental and theoretical study on inhibition behavior of novel quinoline derivatives for the corrosion of mild steel in hydrochloric acid solution. *J. Mol. Liq.* **2017**, *244*, 154–168. [[CrossRef](#)]
14. Jawad, Q.; Hameed, A.; Abood, M.; Al-Amiery, A.; Shaker, L.; Kadhum, A.; Takriff, S. Synthesis and comparative study of novel triazole derived as corrosion inhibitor of mild steel in HCl medium complemented with DFT calculations. *Int. J. Corros. Scale Inhib.* **2020**, *9*, 688–705. [[CrossRef](#)]

15. Al-Amiery, A.; Shaker, L.; Kadhum, A.; Takriff, M. Corrosion Inhibition of Mild Steel in Strong Acid Environment by 4-((5,5-dimethyl-3-oxocyclohex-1-en-1-yl)amino)benzenesulfonamide. *Tribol. Ind.* **2020**, *42*, 89–101. [[CrossRef](#)]
16. Frisch, M.J.; Trucks, G.W.; Schlegel, H.B.; Scuseria, G.E.; Robb, M.A.; Cheeseman, J.R.; Montgomery, J.A., Jr.; Vreven, K.N.K.T. *Pople, Gaussian 03, Revision B.01*; Gaussian Inc.: Pittsburgh, PA, USA, 2003.
17. Koopmans, T. Ordering of wave functions and eigen-energies to the individual electrons of an atom. *Physica* **1933**, *1*, 104–113. [[CrossRef](#)]
18. Ramya, K.; Mohan, R.; Anupama, K.; Joseph, A. Electrochemical and theoretical studies on the synergistic interaction and corrosion inhibition of alkyl benzimidazoles and thiosemicarbazide pair on mild steel in hydrochloric acid. *Mater. Chem. Phys.* **2015**, *149–150*, 632–647. [[CrossRef](#)]
19. Ammal, P.R.; Prajila, M.; Joseph, A. Physicochemical studies on the inhibitive properties of a 1,2,4-triazole Schiff's base, HMATD, on the corrosion of mild steel in hydrochloric acid. *Egypt. J. Pet.* **2018**, *27*, 307–317. [[CrossRef](#)]
20. Garcia-Ochoa, E.; Guzmán-Jiménez, S.; Hernández, J.G.; Pandiyan, T.; Vásquez-Pérez, J.M.; Cruz-Borbolla, J. Benzimidazole ligands in the corrosion inhibition for carbon steel in acid medium: DFT study of its interaction on Fe₃₀ surface. *J. Mol. Struct.* **2016**, *1119*, 314–324. [[CrossRef](#)]
21. Mobin, M.; Aslam, R.; Aslam, J. Non toxic biodegradable cationic gemini surfactants as novel corrosion in-hibitor for mild steel in hydrochloric acid medium and synergistic effect of sodium salicylate: Experimental and theoretical approach. *Mater. Chem. Phys.* **2017**, *191*, 151–167. [[CrossRef](#)]
22. El-Lateef, H.M.A.; Abu-Dief, A.M.; Abdel-Rahman, L.H.; Sañudo, E.C.; Aliaga-Alcalde, N. Electrochemical and theoretical quantum approaches on the inhibition of C1018 carbon steel corrosion in acidic medium containing chloride using some newly synthesized phenolic Schiff bases compounds. *J. Electroanal. Chem.* **2015**, *743*, 120–133. [[CrossRef](#)]
23. Yaro, A.S.; Khadom, A.A.; Wael, R.K. Garlic Powder as a Safe Environment Green Corrosion Inhibitor for Mild Steel in Acidic Media; Adsorption and Quantum Chemical Studies. *J. Chin. Chem. Soc.* **2014**, *61*, 615–623. [[CrossRef](#)]
24. Espinoza-Vázquez, A.; Rodríguez-Gómez, F.J.; Arenas, B.I.V.; Lomas-Romero, L.; Angeles-Beltrán, D.; Negrón-Silva, G.E.; Morales-Serna, J.A. Synthesis of 1,2,3-triazoles in the presence of mixed Mg/Fe oxides and their evaluation as corrosion inhibitors of API 5L X70 steel submerged in HCl. *RSC Adv.* **2017**, *7*, 24736–24746. [[CrossRef](#)]
25. Chuan, L.; Xie, B.; Zou, L.; Zheng, X.; Ma, X.; Zhu, S. Adsorption and corrosion inhibition of mild steel in hydrochloric acid solution by S-allyl-O, O'-dialkyldithiophosphates. *Results Phys.* **2017**, *7*, 3434–3443.
26. Yamin, J.; Sheet, E.; Al-Amiery, A. Statistical analysis and optimization of the corrosion inhibition efficiency of a locally made corrosion inhibitor under different operating variables using RSM. *Int. J. Corros. Scale Inhib.* **2020**, *9*, 502–518. [[CrossRef](#)]
27. Zinad, D.; Hanoon, M.; Salim, R.; Ibrahim, S.; Al-Amiery, A.; Takriff, M.; Kadhum, A. A new synthesized coumarin-derived Schiff base as a corrosion inhibitor of mild steel surface in HCl medium: Gravimetric and DFT studies. *Int. J. Corros. Scale Inhib.* **2020**, *9*, 228–243. [[CrossRef](#)]
28. Zinad, D.; Jawad, Q.; Hussain, M.; Mahal, A.; Mohamed, L.; Al-Amiery, A. Adsorption, temperature and corrosion inhibition studies of a coumarin derivatives corrosion inhibitor for mild steel in acidic medium: Gravimetric and theoretical investigations. *Int. J. Corros. Scale Inhib.* **2020**, *9*, 134–151. [[CrossRef](#)]
29. Alamiery, A.; Mahmoudi, E.; Allami, T. Corrosion inhibition of low-carbon steel in hydrochloric acid environment using a Schiff base derived from pyrrole: Gravimetric and computational studies. *Int. J. Corros. Scale Inhib.* **2021**, *10*, 749–765. [[CrossRef](#)]
30. Pearson, R.G. *Chemical Hardness: Applications from Molecules to Solids*; Wiley-VCH: Weinheim, Germany, 1997.
31. Chattaraj, P.K.; Lee, H.; Parr, R.G. Principle HSAB. *J. Am. Chem. Soc.* **1991**, *113*, 1855–1856. [[CrossRef](#)]